Phonon Dispersion Curves in Wurtzite-Structure GaN Determined by Inelastic X-Ray Scattering

T. Ruf, J. Serrano, and M. Cardona
Max-Planck-Institut für Festkörperforschung, Heisenbergstrasse 1, 70569 Stuttgart, Germany

P. Pavone and M. Pabst
Institut für Theoretische Physik, Universität Regensburg, 93040 Regensburg, Germany

M. Krisch and M. D'Astuto
European Synchrotron Radiation Facility (ESRF), B.P. 220, 38043 Grenoble, France

T. Suski, I. Grzegory, and M. Leszczynski
UNIPRESS, High Pressure Research Center, Polish Academy of Sciences, 01-142 Warsaw, Poland
(Received 30 June 2000)

We have investigated the lattice dynamics of a wurtzite GaN single crystal by inelastic x-ray scattering. Several dispersion branches and phonons at high-symmetry points have been measured, including the two zone-center Raman- and infrared-inactive silent modes. The experiments have been complemented by *ab initio* calculations. They are in very good agreement with our measurements, not only for phonon energies, but also for scattering intensities, thus validating the correctness of the eigenvectors. Other phenomenological and *ab initio* theories exhibit significant differences.

DOI: 10.1103/PhysRevLett.86.906 PACS numbers: 78.70.Ck, 63.20.–e, 78.30.Fs

The wide-band-gap semiconductor GaN is currently of great interest for optoelectronic applications at blue and near-ultraviolet wavelengths, as well as in high-temperature and high-frequency electronics, e.g., high-electron mobility transistors based on the two-dimensional electron gas at the GaN/AlGaN interface. Since the behavior of carriers in such devices, as described by scattering rates, is affected by their interaction with phonons, the lattice-dynamical properties of GaN, i.e., its phonon dispersion and the phonon eigenvectors, are very important and have been studied intensively, mainly by Raman scattering (see, e.g., Refs. [1–4]) and by theory (see, e.g., Refs. [1–3,5–7). Calculations of the phonon dispersion for the zinc blende modification, obtained only under special growth conditions, have recently been extended to the more common wurtzite (hexagonal) structure, stable under ambient conditions. Both phenomenological [1,3] and *ab initio* approaches [6,7] have been published. Unfortunately, tests of these theories have been limited to the comparison with Raman data and are thus incomplete even for the mode *frequencies* at the Brillouin zone center (Γ point). Only in one special case, for the Raman-active coupled E_2 modes, it has also been possible to check predictions for the phonon *eigenvectors* [2]. This essential criterion for the quality of a lattice-dynamical model was tested in GaN made from two different stable nitrogen isotopes.

The main reason for the lack of phonon dispersion information in GaN is that single crystals large enough for inelastic *neutron* scattering do not exist. However, this limitation can now be overcome with inelastic *x-ray* scattering (IXS). With the availability of dedicated beam lines at third-generation synchrotrons, IXS has developed into a powerful alternative for studying *dispersion* effects, i.e., $\omega(\vec{q})$ ($\vec{q} \neq 0$) of elementary excitations in solids [8–10]. As demonstrated here, IXS can even be applied to materials which contain neutron absorbing elements, such as gallium. Using efficient refocusing x-ray optics, spot sizes in the submillimeter range are routinely obtained, and IXS is therefore ideal to investigate very small samples. Another problem in GaN is that even small crystals oftentimes do not have sufficient structural quality. We have overcome this obstacle by using small bulk single crystals obtained from a unique high-pressure growth technique [11]. In order to model the data and to guide the experiments, we have performed *ab initio* lattice-dynamical calculations. The study of the lattice dynamics in wurtzite-structure GaN presented here has been possible only by combining all of these three ingredients. As a result, we present new and important experimental data and an accurate theoretical model. This allows us to identify some significant discrepancies in other models.

GaN crystals were grown at an N_2 pressure of about 1.5 GPa at temperatures of 1500–1600 °C from solution of atomic nitrogen in liquid gallium containing a small amount of Mg [11]. Highly resistive (10^4–10^6 Ω cm), almost dislocation-free (dislocation density less than 10^3 cm^{-2}) platelets of unstrained wurtzite structure GaN were obtained. The GaN sample used in our room-temperature measurements had dimensions of about $2 \times 3 \times 0.2$ mm^3, with the flat side oriented along the uniaxial direction. The widths of rocking scans across Bragg reflections were around 0.007°, indicating excellent crystal quality.

 0031-9007/01/86(5)/906(4)$15.00

The IXS experiment was carried out at beam line ID 28 of the European Synchrotron Radiation Facility in Grenoble. The incident x-ray beam was obtained by a high-resolution backscattering monochromator, utilizing either the silicon (8 8 8) (15.816 keV) or the Si (9 9 9) (17.794 keV) Bragg reflection order [12]. The x-ray beam was focused onto the sample by a toroidal mirror. The spot size was $270 \times 100\ \mu\text{m}^2$ [horizontal $\times$ vertical, full width at half maximum (FWHM)]. The scattered photons were collected by a spherical silicon crystal analyzer operating at the same reflection orders [13]. The FWHM of the instrumental (Lorentzian) resolution function, determined from elastic scattering measurements in a Plexiglas sample, was 44 cm^{-1} (20 cm^{-1}) for the Si (8 8 8) [Si (9 9 9)] reflection. The momentum transfer $Q = 2k_0 \sin(\theta_s/2)$ for the incident photon wave vector k_0 and the scattering angle θ_s was selected by rotating a 7 m long analyzer spectrometer arm in the horizontal scattering plane. The total Q resolution was set to 0.25 nm^{-1}. Energy scans were performed by varying the temperature of the high-resolution monochromator, while the temperature of the analyzer crystal was kept fixed. The conversion from temperature to energy scale is given by $\Delta E/E = \alpha \Delta T$, where α is the thermal expansion coefficient of silicon.

In order to compensate for their much smaller scattering intensities, optical phonons were measured with less resolution and higher flux using the Si (8 8 8) reflection, while acoustic modes were measured with higher resolution and less flux using the Si (9 9 9) reflection. We have systematically performed Stokes–anti-Stokes scans of phonons in order to detect possible zero-point offsets of the energy scale caused by eventual temperature drifts of the monochromator-analyzer system. In most cases, we observed statistical offset variations which did not exceed ± 0.8 cm^{-1}, and no corrections were therefore necessary. From Lorentzian line shape fits to the IXS spectra, phonon frequencies could be determined to within ± 1 cm^{-1} [± 2 cm^{-1}] for excitation with the Si (9 9 9) [Si (8 8 8)] reflection wavelength. The energy widths of the observed peaks were close to that of the exciting x-ray beam.

In order to model the data and to guide the experiments by predictions of scattering intensities, we have performed *ab initio* lattice-dynamical calculations. The plane-wave pseudopotential method within the density-functional and density-functional perturbation theory have been used for determining the structural and dynamical properties, respectively. Nonlocal pseudopotentials (including nonlinear core corrections for Ga) have been generated within the Troullier-Martins scheme [14]. We employed the standard local-density approximation, 28 (14) special points for Brillouin-zone integrations, and basis sets including plane waves up to a kinetic-energy cutoff of 70 (50) Ry for structural (dynamical) calculations. This choice guarantees a convergence of the obtained frequencies within a few percent. The minimization of the total energy with respect to the structural parameters gives $a_{\text{theor}} = 3.145$ Å for the conventional hexagonal lattice constant, $c_{\text{theor}} = 5.113$ Å for the length of the primitive cell (containing two GaN formula units) along the uniaxial direction, and $u_{\text{theor}} = 0.3775$ for the internal parameter (see below for experimental values). Dynamical matrices have been calculated on a regular periodic grid in reciprocal space. Fourier deconvolution on this mesh allows the evaluation of the interatomic force constants needed for calculating frequencies at arbitrary points in reciprocal space [15].

Figure 1 shows IXS spectra of phonons at several high-symmetry points of the Brillouin zone. The number of counts detected during the given accumulation times indicates that the quality of the data varies considerably for different modes, especially between the optic and acoustic frequency regimes. For data taken with the Si (8 8 8) reflection (above 500 cm^{-1}) the incident flux was almost 5 times larger than for the Si (9 9 9) reflection (below 500 cm^{-1}). The frequencies shown in Fig. 1 are compiled in Table I together with Raman data from Ref. [2] and the results of our *ab initio* theory. Although general agreement is quite good, the calculations are systematically somewhat larger than the experimental data. The difference between theory and experiment increases with increasing phonon

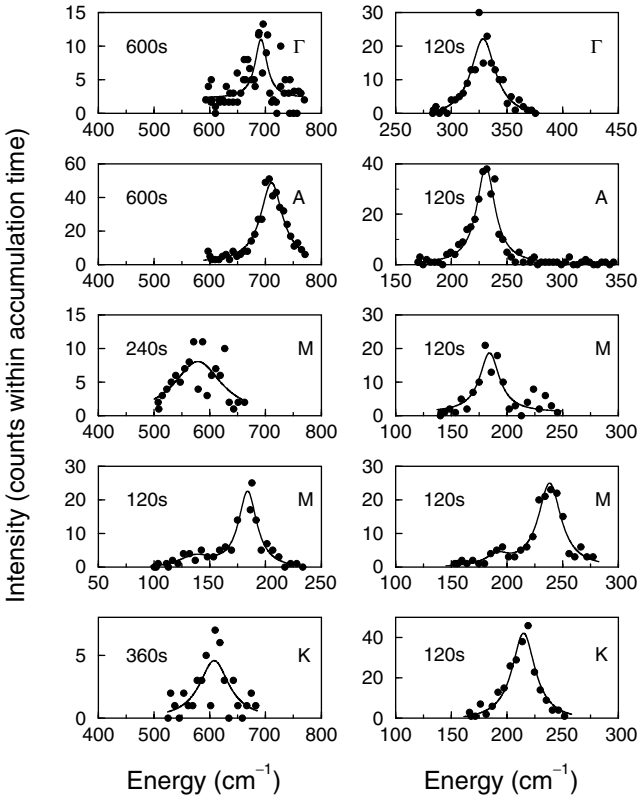

FIG. 1. Inelastic x-ray scattering spectra of phonons in wurtzite-type GaN at several high-symmetry points of the Brillouin zone. The solid lines are Lorentzian line shape fits to the data (filled circles). The accumulation time per data point is indicated for each spectrum.

TABLE I. Frequencies of some high-symmetry phonons in wurtzite-type GaN determined by inelastic x-ray scattering (see Figs. 1 and 2) and Raman scattering (from Ref. [2]) compared to the results of our *ab initio* calculations. All frequencies are given in cm^{-1}; BZE = Brillouin zone edge.

Symmetry point	Mode type	IXS[a]	Raman[b] [2]	Theory[c]
Γ	E_1(LO)		746.6(8)	752.2
Γ	A_1(LO)	729(2)[d]	739.3(4)	751.2
Γ	B_1	692(2)[e]		718.9
Γ	E_2		569.2(2)	581.0
Γ	E_1(TO)		560.0(2)	571.7
Γ	A_1(TO)		533.5(2)	545.2
Γ	B_1	329(1)		338.7
Γ	E_2		144.2(5)	144.7
A	BZE LO	711(2)		735.2
A	BZE LA	231(1)		239.4
M	BZE "A_1(TO)"	576(2)		601.6
M	BZE "E_2"	238(1)		240.7
M	BZE "E_2"	193(1)		199.6
M	BZE TA_z	184(1)		188.3
M	BZE TA_x	137(1)		140.5
K	A_1(TO)-like	614(2)		627.0
K	TA-like	215(1)		215.7

[a]300 K data.
[b]10 K data.
[c]0 K calculation; about 3% larger than our experimental data (see text and caption of Fig. 2).
[d]Extrapolated measurement for $q_z = 0.125\ G_z$. The Raman frequency of 734.0 cm^{-1} at 300 K [3] suggests a difference of about 3 cm^{-1} to the IXS data. Further investigations, also by Raman scattering, are required to clarify its origin.
[e]Extrapolated measurement for $q_z = 0.0625\ G_z$.

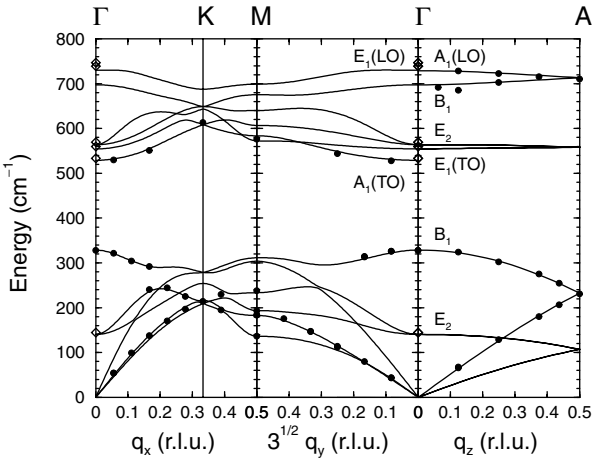

FIG. 2. Phonon dispersion of wurtzite-type GaN along several high-symmetry directions. The filled circles are measured phonon energies from inelastic x-ray scattering; the solid lines are the results of our *ab initio* lattice-dynamical calculation. The theoretical results have been scaled by a factor of 0.97 in order to obtain optimum agreement with the experiment. The open diamonds at $\vec{q} = 0$ are the Raman data from Ref. [2].

frequency. Extensive tables with compilations of calculated phonon frequencies and other measurements at the Γ point can be found in Refs. [2,3,5–7].

Figure 2 shows all IXS data in comparison with the *ab initio* phonon dispersion and the Raman frequencies at Γ [2]. In orthohexagonal notation, we chose as reciprocal lattice units of the crystal momentum $\vec{q} = (q_x, q_y, q_z)$ the reciprocal lattice vectors $G_x = 4\pi/a$, $G_y = 4\pi/(\sqrt{3}\,a)$, and $G_z = 2\pi/c$. Lattice constants $a = 3.189$ Å and $c = 5.185$ Å were determined at ID 28 for the sample investigated. In order to obtain optimum agreement with the experimental data, the theoretical results were scaled by a constant factor of 0.97. This correction is well within the overall reliability of the calculations and even somewhat less than the factor of 0.95 used in a recent study of wurtzite CdS [16].

From the theoretical eigenvectors we also calculated scattering intensities (selection rules) and identified suitable scattering geometries, i.e., the reciprocal lattice vectors $\vec{G}$ for which the strongest signals should occur. We found excellent agreement between these predictions and the observed phonons. For example, phonons of the B_1-related branches along Γ-A were measured with odd-parity index $\vec{G} = (0, 0, 5)$, while those of the A_1-related branches could be obtained only with the even-parity index reciprocal lattice vectors $\vec{G} = (0, 0, 4)$ or $(0, 0, 6)$. For $\vec{G}$ with the opposite-parity indices, respectively, no intensity was observed. This proves that our theory also predicts the correct eigenvectors.

One main result of our IXS study is the observation of the two *silent* B_1 modes at Γ (see Table I), since these data can be neither obtained by first-order Raman nor by infrared spectroscopy. IXS even allows us to measure their dispersion. These phonons are rather important input parameters for fits of phenomenological models. Their energy at Γ determines whether mode anticrossings with other dispersion branches occur inside the Brillouin zone. In CdS, for example, insufficient information on the B_1 frequencies has been identified as the origin of strong errors in phenomenological lattice-dynamical models [16]. The energy difference between the higher-energy B_1 mode and A_1(LO) at Γ in wurtzite GaN is a measure of the dispersion of the longitudinal-optic branch along Γ-A-Γ which corresponds to the Γ-L dispersion in the zinc blende modification, "backfolded" onto the shorter Brillouin zone of the wurtzite unit cell along q_z. The frequencies of the higher- and lower-energy B_1 modes at Γ should thus be very close to those of the longitudinal optic and acoustic modes at L in zinc blende GaN, respectively, for which no experimental data are yet available. However, values of 720 and 345 cm^{-1} have been calculated [5], in good agreement with our results.

From IXS we find an energy difference between A_1(LO) and B_1 of 37 cm^{-1}, in good agreement with our theory (32 cm^{-1}) and a recent, rather similar, *ab initio* study

(43 cm^{-1}), performed independently [7]. The phenomenological model of Ref. [1] overestimates this splitting by a factor of 2; that of Ref. [3] underestimates it by a factor of 6. In both cases this discrepancy goes along with significant differences of the phonon dispersion in high-symmetry directions as compared to our results. For example, a clear separation between the singlet LO-derived modes and the doublet TO-related phonons is predicted in Ref. [1], while heavy mixing between these states is expected according to Ref. [3]. The differences between our results and those of Ref. [1] are less pronounced in the acoustic regime. Significant differences, however, appear in comparison with the dispersion of Ref. [3].

A frequency of 320 cm^{-1} for the lower-energy B_1 mode at Γ has been derived from second-order Raman spectra in Ref. [1]. Our direct measurement, however, gives a larger frequency. Similarly, the value of 300 cm^{-1} for this mode, inferred from first-order Raman scattering in disordered GaN samples in Ref. [4], is lower than our data. Since the scattering intensity of this silent mode should still be very small, even when it becomes symmetry-allowed in second-order Raman scattering or activated by disorder, these observations can be reconciled by assuming that in both cases [1,4] features of the phonon density of states, with a maximum at somewhat lower energies, rather than the B_1 mode directly at Γ have been observed.

The results of our *ab initio* calculation, confirmed by the IXS data, and those of Ref. [7] are quite similar. This is not surprising given the fact that the same approach has been used. However, the *ab initio* results of Ref. [6], obtained by a frozen-phonon-like method implemented using the commercial Vienna *ab initio* simulation package, based on the augmented plane-wave approach, are distinctly different in some aspects of the dispersion. While all three theories agree quite well for the Γ-K-M-Γ directions, i.e., in the hexagonal plane, Ref. [6] predicts a crossing of the A_1(LO)-A and upper B_1-A branches about halfway between Γ and A. Furthermore, the A_1(LO)-A dispersion line exhibits a characteristic "undershooting" near the A point. According to this calculation, the (highest-energy) A point is lower than the B_1 mode at Γ by about the A_1(LO)-B_1 splitting. Consequently, the B_1-A line in Ref. [6] is curved towards lower frequencies, in clear disagreement with our IXS data and the present calculations. Furthermore, the second highest A point in Ref. [6] has a larger energy than both the E_2 and E_1 modes at Γ with which it is connected by two twofold degenerate dispersion branches. These anomalies for the highest Γ-A branches occur neither in any other calculation nor in any wurtzite material for which experimental data are available [10,16,17]. Usually, the A point frequencies of these branches are located near the average frequencies of the corresponding Γ point modes, as one would expect for a smoothly decreasing "unfolded" Γ-L dispersion in the corresponding zinc blende modifications. We conjecture that the higher spatial frequencies present in the Γ-A dispersion branches of Ref. [6] arise from an incorrect treatment of far-reaching interactions. The dispersion along A-H-L-A is also strongly affected by this problem. This is probably due to the somehow artificial procedure used in Ref. [6] for deducing force constants for wurtzite GaN from calculations performed on rhombohedral supercells. In contrast, the present calculations and those of Ref. [7] directly address the wurtzite structure. Defying some current trends which claim that the undoubtedly powerful modern computational methods might make experiments unnecessary, our results demonstrate that *measurements* are indeed indispensable to test not only theoretical phenomenological models but also the approximations and procedures used in *ab initio* calculations.

We thank W. Kress for a critical reading of the manuscript. J. S. acknowledges support from Max-Planck-Gesellschaft and Ministerio de Educación y Ciencia (Spain) through the Plan Nacional de Formación del Personal Investigador.

[1] H. Siegle *et al.,* Phys. Rev. B **55**, 7000 (1997).
[2] J. M. Zhang *et al.,* Phys. Rev. B **56**, 14 399 (1997).
[3] V. Yu. Davydov *et al.,* Phys. Rev. B **58**, 12 899 (1998).
[4] N. Wieser *et al.,* Phys. Status Solidi (b) **216**, 807 (1999).
[5] K. Karch *et al.,* Phys. Rev. B **57**, 7043 (1998).
[6] K. Parlinski and Y. Kawazoe, Phys. Rev. B **60**, 15 511 (1999).
[7] C. Bungaro *et al.,* Phys. Rev. B **61**, 6720 (2000).
[8] M. Schwoerer-Böhning *et al.,* Phys. Rev. Lett. **80**, 5572 (1998).
[9] M. Holt *et al.,* Phys. Rev. Lett. **83**, 3317 (1999).
[10] M. Schwoerer-Böhning *et al.,* Phys. Status Solidi (b) **215**, 177 (1999).
[11] I. Grzegory *et al.,* J. Phys. Chem. Solids **56**, 639 (1995).
[12] R. Verbeni *et al.,* J. Synchrotron Radiat. **3**, 62 (1996).
[13] C. Masciovecchio *et al.,* Nucl. Instrum. Methods Phys. Res., Sect. B **111**, 181 (1996); **117**, 339 (1996).
[14] N. Troullier and J. L. Martins, Phys. Rev. B **43**, 1993 (1991).
[15] P. Giannozzi *et al.,* Phys. Rev. B **43**, 7231 (1991).
[16] A. Debernardi *et al.,* Solid State Commun. **103**, 297 (1997).
[17] F. Widulle *et al.,* Physica (Amsterdam) **263/264B**, 420 (1999).